Fragility analysis of a bridge substructure under Level-1 earthquake and its application to determination of safety factors

M. M. Hoque*, Y. Seshimo**, M. Tsunekuni**, Y. Okui***, T. Sugiyama****

*Doctoral Student, Dept. of Civil and Environmental Eng, Saitama University, Saitama-shi, Saitama 338-8570
**Advanced Engineering Operation Center, Tokyo Electric Power Services, Co. Ltd. Tokyo
***Dr. Eng., Assoc. Professor, Dept. of Civil and Environmental Eng, Saitama University, Saitama-shi, Saitama 338-8570
****Dr. Eng., Professor, Dept. of Civil Engineering, Yamanashi University, Kofu

Monte Carlo Simulation technique is employed to construct fragility curves of a highway bridge substructure under Level-1 earthquake ground motion. Elastic limit criteria for pier, footing, and pile body are considered in terms of flexure, shear, and combination of flexure and axial stresses in concrete and tensile stress in reinforcing steel. In addition, for pile foundation, the axial load bearing capacity and horizontal stability of pile are considered. Fragility analysis results indicate different levels of safety margins for different design criteria and members. Statistical tests of goodness-of-fit show that all fragility curves follow normal distribution. Lifetime failure probability is estimated by convoluting the fragility curves with the seismic hazards of the 50-years extreme values of earthquake ground motions. Finally, relationships between member safety factors and the failure probability are presented.
Key Words: *Fragility, uncertainty and variability, safety margin, failure probability*

1. Introduction

The earthquake resistant structural design methodology employed in recent seismic design codes calls for ensuring different levels of performance depending on characteristics of earthquake ground motion. In fact, design specifications[1-3] define two levels of ground motion, namely Level-1 (L1) and Level-2 (L2) based on the probability of occurrence and the extent of consequences of such events. According to earthquake resistant design code in Japan[3], L1 earthquakes are of moderate magnitude and may occur several times during the service life of a structure, while the earthquakes defined as L2 are of much larger magnitude and much lower occurrence probability than those of L1. Therefore, a structure may not encounter L2 earthquakes during its lifetime. According to these specifications, designed structures are required to perform adequately in resisting L1 earthquakes without any damage. Hence, due to L1 earthquakes, the response of the structures is required to be within the elastic limit so that any residual deformation does not remain in the structures. In the case of L2 earthquakes, the designed structure, however, should not collapse even though the occurrence of limited damage is permitted.

To design highway bridges against L1 earthquakes, Specifications for Highway Bridges (SHB)[4] uses the seismic coefficient method, whereas the ductility design method is employed for a bridge capable of resisting L2 earthquakes. In order to design bridges meeting L1 performance level, SHB[4] uses the allowable stress design (ASD) method as a design basis. In ASD, safety is ensured by a single safety factor that is derived from experience and/or engineering judgments. However, this traditional design method has a number of well-recognized and significant limitations. For example, it lacks the flexibility to adjust a constant safety margin for different load cases and load combinations. Very often, the same numerical safety factor in ASD approach may imply different levels of the safety margin in actual design. Another significant source of ambiguity lies in the relationship between the safety factor and the underlying level of risk. A larger safety factor does not always imply a lower level of risk, since the effect of safety factor can be negated by the presence of many uncertainties in design variables. In order to overcome these ambiguities, it is indispensable to improve the traditional design approach to deal adequately with the uncertainties.

As an alternative to this approach, a current trend in developing design codes encourages to use load and resistance factor design (LRFD) method based on reliability analyses[5-8]. In LRFD, safety factors are assigned to both resistance and load separately. Accordingly, we have to consider uncertainties in load and resistance separately. One of the ways to assess the uncertainty only in resistance is to use fragility curves. Fragility curves represent the probability of a structure being damaged beyond a specific damage state for various levels of earthquake ground motions. Seismic probabilistic risk assessment[9], vulnerability information[10,11], and risk based policy development[12] for designing structures can be developed from the fragility curves. Moreover, they may be utilized to analyze, to evaluate, and to improve the seismic safety margin of structural systems[13]. Recently, Yamazaki *et al.*[14] constructed sets of empirical fragility curves for highway bridges based on actual damage data from the 1995 Hyogoken-Nanbu earthquake. Later on, Kim and Feng[9], Karim and Yamazaki[10], and Shinozuka *et al.*[15] developed

analytical fragility curves for highway bridge pier by numerical simulation of seismic responses.

With this background, the present work aims to construct fragility curves of a highway bridge substructure subjected to L1 earthquake ground motions and to discuss the safety margin of different design criteria and members. Monte Carlo Simulation (MCS) is employed to take account of uncertainty of the design variables adequately. Statistical data of the random variables are collected from published literatures. In conventional studies[9-11], the fragility curves were approximated with lognormal distribution. To verify adequacy of the approximation of fragility curves with lognormal distribution, statistical test has been carried out. In addition, lifetime failure probabilities are calculated by convoluting the fragility curves with the seismic hazards for 50 years extreme values of ground motion records. Finally, relationships between the failure probability and member safety factors of designing highway bridges under L1 earthquakes are presented.

2. Elastic limit criteria for Level-1 earthquake

In order to meet the seismic performance criteria for Level-1 earthquake, the structures are required to behave elastically. Accordingly fragility of the elastic limit for individual parts or failure modes in a bridge substructure will be developed in subsequent chapter. To this end, first, we adapt the design equations specified in SHB[4, 16] for L1 earthquake as a criterion for elastic limit. Since our main concern of this study is to propose a rational method to determine safety factors, the accuracy of the design equations themselves will not be discussed in this paper.

In SHB[4] for L1 seismic design, ASD is adopted as mentioned before, and a general form of design equations for an elastic limit criterion is expressed as

$$\frac{R_n}{FS} \geq S_d + S_e \tag{1}$$

where R_n= nominal resistance; FS= factor of safety; S_d and S_e=design values of dead load effect and seismic load effect, respectively.

Since we will discuss uncertainty only in resistance in terms of fragility curves and investigate safety factors on the basis of LRFD format, we rewrite the design equation into simplified LRFD format:

$$\frac{1}{\gamma_b} R\left(\frac{f_k}{\gamma_m}\right) \geq S_d + S_e \tag{2}$$

where γ_b and γ_m =member and material safety factors, respectively; f_k =characteristic value of material strength; R=resistance against a particular mode of failure. In this simplified LRFD format, the importance factor and the safety factors for analytical method are assumed to be unity for simplicity.

Table 1 shows the list of design equations employed in construction of fragility curves. These design equation are classified into four parts: pier, footing, pile body and pile foundation. The checking points of individual design equations are shown in Fig. 1. Except for pile foundation, all design equations are expressed in terms of stresses including the material safety factors for steel γ_{ms} and for concrete γ_{mc}. When rewriting these design equations from the ASD format into SHB, the following relationships between allowable stresses and design strengths are used:

$$\sigma_{ca} = \frac{1}{2} f_{cd} = \frac{1}{2} \frac{f_{ck}}{\gamma_{mc}} \tag{3}$$

$$\tau_{ca} = \frac{c_e c_{pt}}{1.67} f_{sd} = \frac{c_e c_{pt}}{1.67} \left\{ 0.2 \left(\sqrt[3]{\frac{f_{ck}}{\gamma_{mc}}} \right) \right\} \tag{4}$$

where σ_{ca} and τ_{ca} are the allowable stresses for bending compression and shear, respectively; f_{cd} and f_{ck} denote the design and characteristic compressive strengths of concrete; f_{sd} stands for design shear strength of plain concrete; c_e and c_{pt} denote the correction factors with respect to the effective depth of a member section and reinforcement ratio of the main tensile reinforcement.

The allowable stress for reinforcing steel σ_{sa} can be written:

$$\sigma_{sa} = \frac{f_{yk}}{\gamma_{ms}} \tag{5}$$

where f_{yk}=characteristic yield strength for reinforcing steel.

For foundation, the allowable axial load bearing capacity of pile for push-in P_{push} and pull-out P_{pull} are defined by

$$P_{push} = \frac{q_d A_{tip} + U \sum L_i f_s}{3} - W \tag{6}$$

$$P_{pull} = \frac{U \sum L_i f_s}{2} + W_s - W \tag{7}$$

where q_d and f_s are the tip resistance and side frictional resistance of pile; U denote peripheral length of a pile section; A_{tip} stands for cross-sectional area of pile tip; L_i is the thickness of soil layer; and W and W_s indicate weight of a pile body and weight of soil replaced by the pile body.

The allowable displacement at pile head is considered as 1% of the pile length.

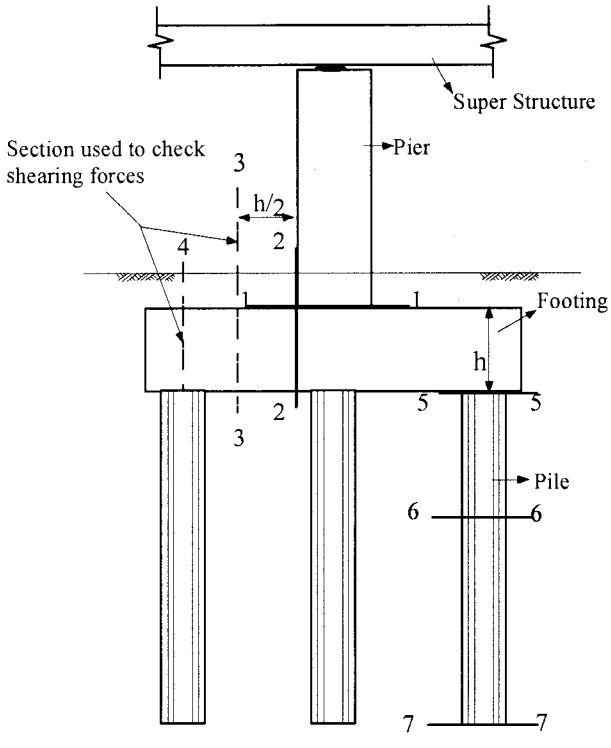

Fig. 1 Checking points of design equations

Table 1 Design equations considered in construction of fragility curves

Part of substructure	Checking point	Design criteria	Design equations
Pier	Section 1-1	Tensile stress in reinforcing bar	$g_{p1} = \frac{1}{\gamma_{bp_1}}\left(\frac{f_{yk}}{\gamma_{ms}}\right) - \sigma_{tr}$
		Bending compressive stress in concrete	$g_{p2} = \frac{1}{\gamma_{bp_2}}\left(\frac{1}{2}\frac{f_{ck}}{\gamma_{mc}}\right) - \sigma_{bc}$
		Shear stress in concrete	$g_{p_3} = \frac{1}{\gamma_{bp_3}}\left[\frac{c_e c_{pt}}{1.67}\left\{0.2\left(\sqrt[3]{\frac{f_{ck}}{\gamma_{mc}}}\right)\right\}\right] - \tau_c$
Footing	Section 2-2	Tensile stress in reinforcement	$g_{f1} = \frac{1}{\gamma_{bf_1}}\left(\frac{f_{yk}}{\gamma_{ms}}\right) - \sigma_{tr}$
		Bending compressive stress in concrete	$g_{f2} = \frac{1}{\gamma_{bf_2}}\left(\frac{1}{2}\frac{f_{ck}}{\gamma_{mc}}\right) - \sigma_{bc}$
	Section 3-3 or section 4-4	Flexural shear stress in concrete	$g_{f3} = \frac{1}{\gamma_{bf_3}}\left[\frac{c_e c_{pt}}{1.67}\left\{0.2\left(\sqrt[3]{\frac{f_{ck}}{\gamma_{mc}}}\right)\right\}\right] - \tau_c$
Pile body	Section 5-5 or section 6-6	Tensile stress in reinforcement	$g_{ps_1} = \frac{1}{\gamma_{ps_1}}\left(\frac{f_{yk}}{\gamma_{ms}}\right) - \sigma_{tr}$
		Bending compressive stress in concrete	$g_{ps2} = \frac{1}{\gamma_{ps_2}}\left(\frac{1}{2}\frac{f_{ck}}{\gamma_{mc}}\right) - \sigma_{bc}$
	Section 5-5	Shear stress in concrete	$g_{ps_3} = \frac{1}{\gamma_{ps_3}}\left[\frac{c_e c_{pt}}{1.67}\left\{0.2\left(\sqrt[3]{\frac{f_{ck}}{\gamma_{mc}}}\right)\right\}\right] - \tau_c$
Pile foundation	Section 7-7	Axial force of push-in	$g_{pf1} = \frac{1}{\gamma_{bpf_1}} P_{push} - P_{n1}$
	Head of pile	Axial force of pull-out	$g_{pf2} = \frac{1}{\gamma_{bpf_2}} P_{pull} - P_{n2}$
		Horizontal displacement	$g_{pf3} = \frac{1}{\gamma_{bpf_3}}\delta' - \delta$

Note:
The subscripts *p, f, ps*, and *pf* of g and γ_b are used to indicate pier, footing, pile structure, and pile foundation, respectively; P_{n1} denotes axial force of a pile in push-in; P_{n2} stands for axial force of a pile in pull-out; and δ is the horizontal displacement at pile head. Section 6-6 of Fig. 1 represents the point on the embedded portion of the pile body where maximum bending moment occurs if the connection between the pile and the footing is considered as hinge.

3. Model Bridge Substructure

The model bridge substructure shown in Fig. 2 is adopted from a reference manual of seismic design[17]. As with conventional design procedure, only a set of the substructure is considered, which consists of a reinforced concrete (RC) pier, RC footing, and cast-in-place RC piles. The effect of superstructure is modeled as an inertia force of 6340 kN, acting at the center of gravity of the super structure, in the longitudinal direction as shown in Fig. 2(b). The dimensions of the model bridge and the amount of reinforcement are designed in accordance with SHB[4,16]. The material parameters used in designing are listed in Table 2. According to SHB[16], the foundation system i.e. a footing supported by a group of piles is modeled as an elastic frame supported by axial and radial springs of constant stiffness. The axial spring constants are computed by means of an estimation formulae based on previous vertical load test data as mentioned in SHB[4] and the radial spring constants of piles are estimated using the modulus of subgrade reaction and based on the theory of a beam on elastic floor. The bottom ends of the piles are assumed to reach the dense sand stratum. For simplicity, the ground condition is considered homogeneous. However, the random variability of the soil properties is considered.

4. Monte Carlo Simulation

For simplicity and robustness, this study employs the

Table 2 Design strength of materials

Part of substructure	Concrete	Reinforcing steel (yielding)
Pier and footing	20.6 N/mm^2	295 N/mm^2
Pile	23.6 N/mm^2	95 N/mm^2

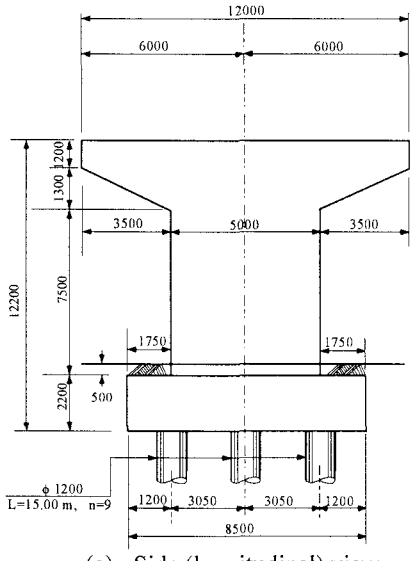

(a) Side (longitudinal) view

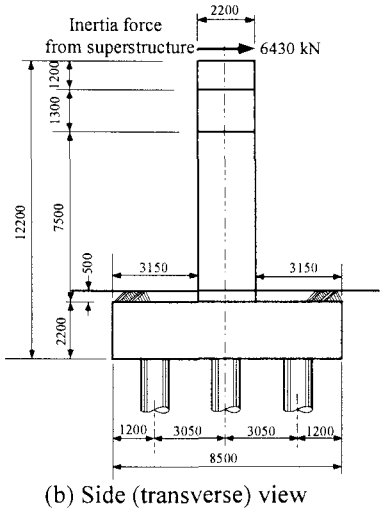

(b) Side (transverse) view

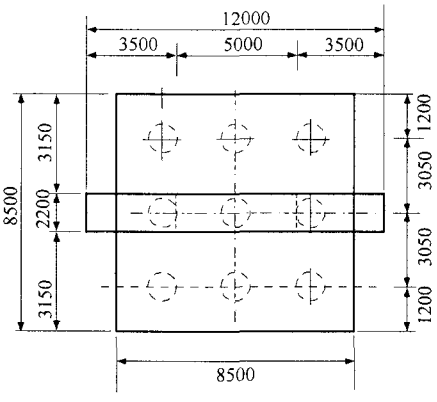

(c) Top view

Fig. 2 Model bridge substructure

simplest form of Monte Carlo Simulation (MCS) denoted as Direct Monte Carlo Simulation (D-MCS). Here, random values of each variable are generated independently. Structural responses e.g. stress in reinforcing steel and concrete are evaluated for all the realizations of random variables. For specific ground acceleration a, the probability of damage P i.e., probability of exceeding elastic limit criteria, is estimated by

$$P(x;a)=\sum_{n=1}^{nSim} I[g(x)\le 0]w_n(a) \tag{8}$$

where x=random variables; $w_n(a)$= weight of the sample; $nSim$= sample size; $g(x)$= the limit state function and $I[\ ]$= an indicator function which equals 1 if [ ] is 'true' and 0 if [ ] is false. In D-MCS, all weights are constant and equal to $1/nSim$.

A total of 350 ground acceleration values starting from 0.01 with an increment of 0.01g are used in this study. The points on the fragility curves are worked out by repeating the aforementioned estimating procedure for all the ground acceleration values. Fig. 3 shows the flow chart of Monte Carlo technique used in this study to construct fragility curves.

4.1 Statistical Properties

The uncertainty and variability of the design parameters related to resistance are considered in this study. However, the uncertainties concerning section dimensions such as the height and width of a section, the depth of concrete cover and the amount of reinforcement are ignored due to less significant effects[18]. Table 3 shows the characteristics of all considered statistical variables, which have been collected from several previous studies. The fundamental random variables belong to three basic materials: concrete, soil, and reinforcing steel. For concrete, the unit weight, compressive strength and modulus of elasticity are considered as the fundamental random variables. The fundamental random variables related to reinforcing steel are yielding strength and modulus of elasticity. Unit weight, SPT N-value, side friction and end bearing resistance of a pile are considered as the fundamental random variables for soil.

(1) Concrete

For the compressive strength of concrete, normal probability distribution has been considered by many investigators[6,15]. In this study, the construction quality is assumed as well controlled and the coefficient of variation (COV) is selected as 0.11[19].

The mean strength of concrete is often related to its characteristic strengths, and that relationship is shown in Fig. 4. Hence, the relationship between the mean and characteristic strength can be written as

$$f_{ck}=f_{cm}(1-k_n V_c) \tag{9}$$

where f_{cm} and f_{ck} = mean and characteristic values compressive strength of concrete; V_c=COV for concrete strength; k_n = a factor depending on the type of statistical distribution. For the normal distribution and 5% level of significance k_n

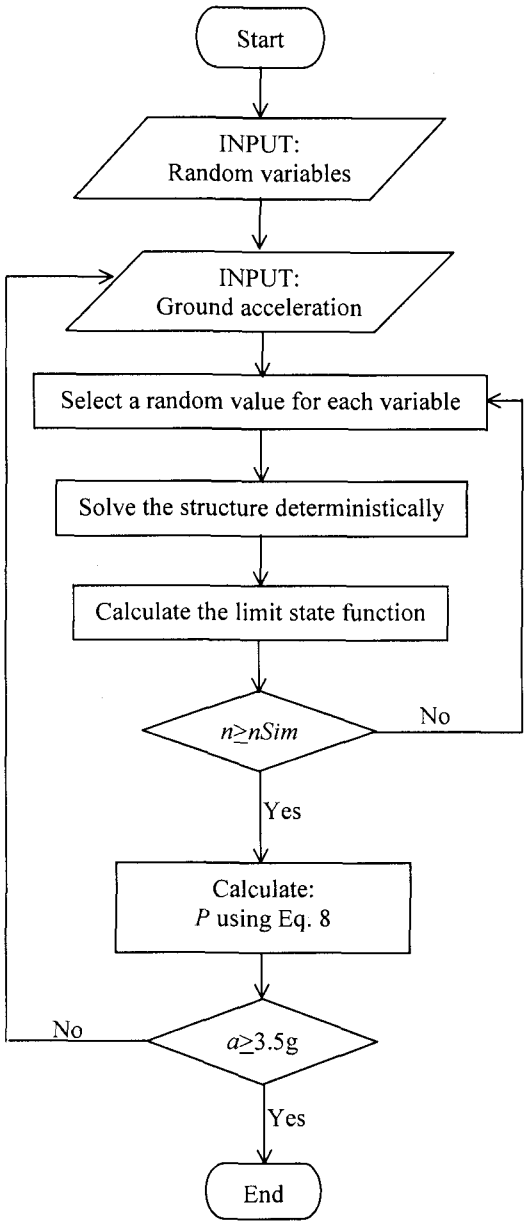

Fig. 3 Flow chart of Monte Carlo Simulation technique used to construct fragility curves

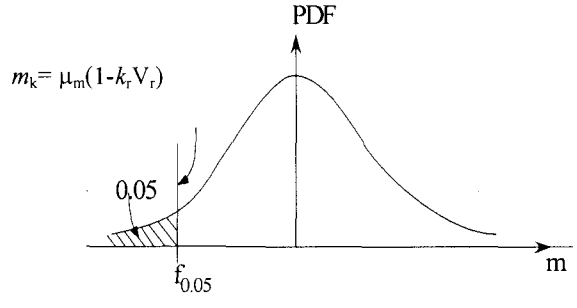

Fig. 4 Relationship between mean value and characteristic value

equals 1.645 and the Eq. (9) turns into

$$f_{ck} = f_{cm}(1-1.645V_c) \tag{10}$$

Using the design value of compressive strength of concrete specified by SHB[16], mean value of the compressive strength is estimated. Taking into consideration of all these information, the statistical values indicated in Table 3 are employed for the present analysis.

(2) Reinforcing steel

Different statistical distribution for the yield strength of reinforcing steel has been proposed by different researchers: Low and Hao[20] (normal); Galambos and Ravindra[21] (log-normal), and Mirza and McGregor[22] (beta distribution). However, the normal distribution is more appropriate for yield strength of reinforcement at 95% confidence level[23]. Hence, the normal distribution for yield strength of reinforcing steel is used in this study. Galambos and Ravindra[21] recommended a COV equal to 8-12%. Considering progress of manufacturer's control over quality with time, a lower value of COV i.e. 8% is selected for this study.

From the characteristic value of yield strength as specified by SHB[16], mean value f_{ym} is evaluated considering that characteristic value at 5% fractal. The relationship is defined by

$$f_{ym} = \frac{f_{yk}}{1-1.645V_r} \tag{11}$$

where f_{yk} is the characteristic yield strength and V_r is the COV of yield strength of reinforcing steel.

(3) Soil properties

In SHB[16], SPT N-values is used to estimate the side friction, and bearing resistance of piles, and the spring constants of the ground. Kulhway[24], Phoon[25], and Rackwitz[26] summarized the nature of distributions and COV ranges of soil properties for different types of deposits. They reported that COV of SPT N-values lies within the range of 15-45%. It is worthy to note that the average of SPT N-values along the depth, instead of N- values at points for a certain significant depth, controls the side friction, end bearing resistance of a pile and the spring constants of the ground. Honjo *et al.*[27] and Vanmarcke[28] recommended reducing the variance SPT N-values averaged over depth. Kulhway[24] and Phoon[25] proposed a COV of SPT N-value 0.3 for sandy layer. Hence, SPT N-value is assigned to 0.3 in this study. Normal distribution is assumed for the averaged SPT N- values, because it is more likely to follow the normal distribution following the central limit theorem.

Honjo *et al.*[29] considered a relationship between SPT N-values and side friction or end bearing resistance of piles after analyzing 350 pile load test results. They also evaluated the uncertainty of side friction and end bearing resistance of piles. Using the χ^2 fitness test results, they confirmed whether normal or lognormal distribution is valid for representing the respective uncertainties with a significance level of 5%. However, they introduced two new random variables so called biases, for representing the uncertainty in the evaluation of pile side friction and end bearing resistance. The mean values, used by the above authors, of these parameters are evaluated as 1.07 and 1.12 with COV 0.46 and 0.63, respectively. For simplicity, without considering additional biased parameters, this study uses the side friction and end-bearing resistance of pile as normally distributed random variables with COV of 55% and 43%, respectively.

Table 3 Selected Statistical Properties of Random Variables

Basic material	Fundamental Random Variables	Type of Distribution	Mean value	COV (%)	References
Concrete	ρ_c	Normal	23.5 kN/m^3	11	Al-Harthy and Frangopol[30]
	f_{ck}	Normal	25 N/mm^2	11	Mirza *et al.*[19]
	E_c	Normal	26 kN/mm^2	8	Mirza *et al.*[19]
Reinforcing bars	f_{yk}	Normal	360 N/mm^2	8	Galambos and Ravindra[21]
	E_r	Normal	201 kN/mm^2	11	Mirza and McGregor[22]
Soil	ρ_s	Normal	18 kN/m^3	7	Kulhawy[24], Duncan[31]
	ρ_{sf}	Normal	17 kN/m^3	8	Rackwitz[26]
	SPT N-value	Normal	15*	30	Kulhway[24], Phoon[25]
	f_s	Normal	175* kN/m^2	55	Honjo *et al.*[29]
	q_d	Normal	3800* kN/m^2	45	Honjo *et al.*[29]

Notes:
1) * : these values are estimated
2) ρ_c, ρ_s, and ρ_{sf} : unit weight of concrete, original soil and fill soil, respectively; SPT N: standard penetration blow count; f_{ck} : characteristic compressive strength of concrete E_s : modulus of elasticity of reinforcing steel; E_c: modulus of elasticity of concrete; f_{yk} : characteristic yield strength of reinforcing steel; f_s : side resistance of pile; and q_d :end bearing resistance of pile.

5. Convergence of fragility curves

Convergence of the fragility curves is investigated to get the minimum number of simulation cycles for MCS so that it can be used in constructing fragility curves. First of all, fragility curves are constructed for an arbitrary number of simulation cycles. Then the simulated fragility curves are fitted to normal and lognormal distribution function by a nonlinear least square method[32]. Simultaneously, a statistical test of goodness-of-fit has been conducted to find out the distribution that is to be followed by the fragility curves. Later on, the number of simulation cycles is changed and the same process is repeated for different numbers of simulation cycles. However, for presentation purpose, the convergence and the test of goodness-of-fit of the fragility curves are described in two different chapters. According to the test of goodness-of-fit, which will be described in detail in chapter 6, the fragility curves are found to follow normal distribution, and therefore these curves can be expressed by their mean values and standard deviations. In the following, the convergence of fragility curves is considered as the convergence of the parameters and checked for all members. Although the convergence is checked for all members, the results for pile foundation are presented for illustrations that are shown in Fig. 5.

It can be seen from Fig. 5 that at lower values of simulation cycles, the statistical parameters fluctuate, while after a certain number those become stable indicating the convergence of the fragility curves. As an example, the mean values of fragility curves for pier converge after 1000 cycles simulation that is not shown here, while fragility curves of pile foundation, as shown in Fig. 5a, are found to converge at around 1500 realizations.

The larger number of realization is needed for pile foundation due to larger variability of the random variables affecting the fragility curves, which will be discussed in detail in chapter 7. Fragility curves for all the design criteria consi-

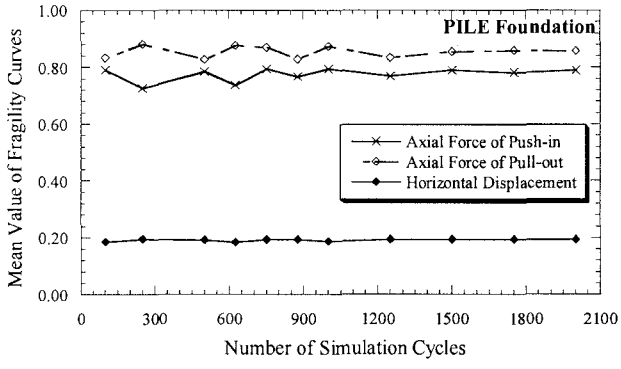

(a) Mean values

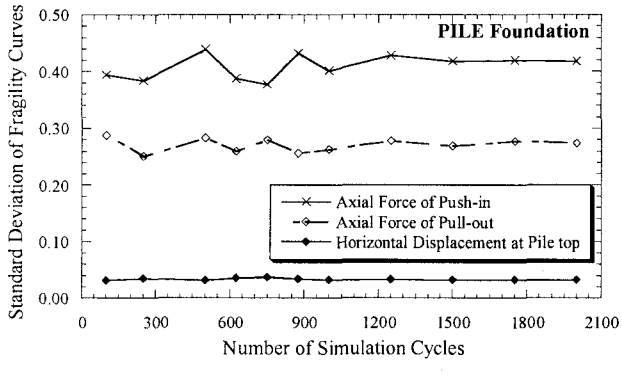

(b) Standard deviations

Fig. 5 Convergence of fragility curves for pile foundation

dered in this study are found to converge at 1500 cycles. Hence, 1500 simulation cycles is considered as minimum for convergence and will be utilized subsequently for developing fragility curves.

In order to ascertain the tail of the distribution, life time failure probability for different design criteria and members have been estimated for different number of simulation cycles and found to converge at or before 1500 cycles.

6. Goodness-of-fit

The Kolmogrov-Smirnov (K-S) test has been conducted to verify adequacy of the approximation that fragility curves follow lognormal and normal distributions and to know the level of significance for these approximations. The test is based on the maximum difference between the simulated and assumed cumulative distribution function (CDF) of the ordered data expressed as,

$$D_n = \max\left|F_X(a_i) - S_n(a_i)\right| \tag{12}$$

where $F_X(a_i)$ is the theoretical CDF of assumed distribution at the i-th simulation of the acceleration a_i, and $S_n(a_i)$ denotes the corresponding CDF of the simulated samples. D_n is a random variable and its distribution depends on the sample size n. The CDF of D_n can be related to the level of significance (LS) α as,

$$P\left(D_n \le D_n^{\alpha}\right) = 1 - \alpha \tag{13}$$

and the critical values for different α are obtained from text book of statistics[33]. If the maximum difference D_n is less than or equal to critical value D_n^{α}, one can accept the assumed distribution at the LS α. Since D_n^{α} depends on the number of data, the K-S tests are carried out for different sample sizes by changing the increment of ground acceleration. In this paper only results for an increment of ground acceleration 0.01g are shown due to limitations of space.

Fig. 6 presents the results of K-S tests for all design criteria considered in this study. For pier, it is seen from Fig. 6(a) that the approximation of fragility curves with lognormal distribution is valid with α=1% and that with normal distribution is accepted with α>20%

It is clear from Fig. 6(b), 6(c) and 6(d) that all design criteria of other members are not fitted to lognormal distribution, because the maximum differences between two CDF exceed the critical values. In contrast, the normal distribution function is acceptable with α=5% in the present simulation.

A reason for it might be due to assumption of normal distribution for all random variables. When the limit state equation is a linear function of the random variables those are normal, then the probability of exceeding the limit states i.e. the probability of damage against ground acceleration will be normal.

7. Fragility Curves

Fig. 7 shows the fragility curves of the bridge substructure subjected to L1 earthquake ground motions. One can easily see the qualitative differences in the locations and variability of fragility curves for different design criteria. In order to quantify the differences, the mean values and the standard deviations of the fragility curves are evaluated considering those as normally distributed. Fig. 8 shows the statistical parameters of these curves together with the list of random variables affecting each design criterion. In this fig-

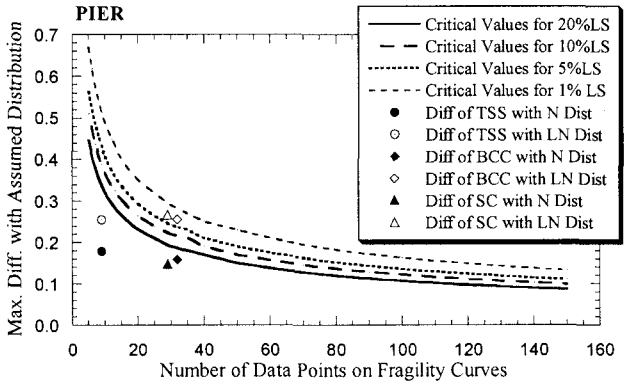

(a) Pier

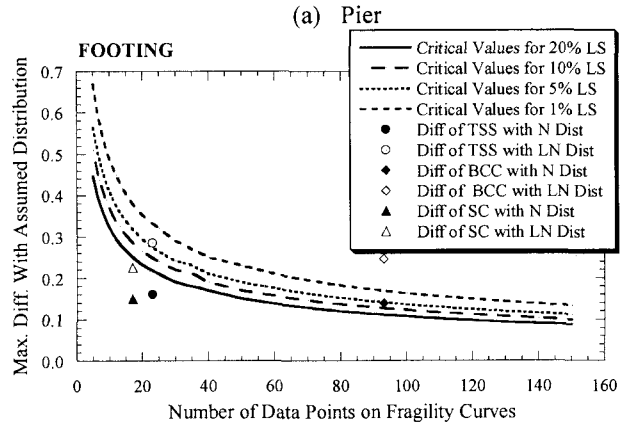

(b) Footing

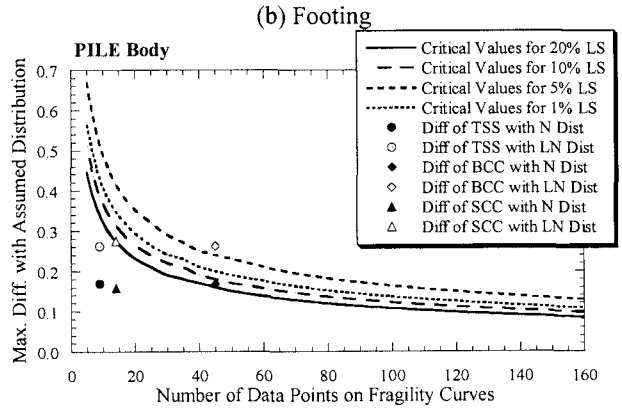

(c) Pile body

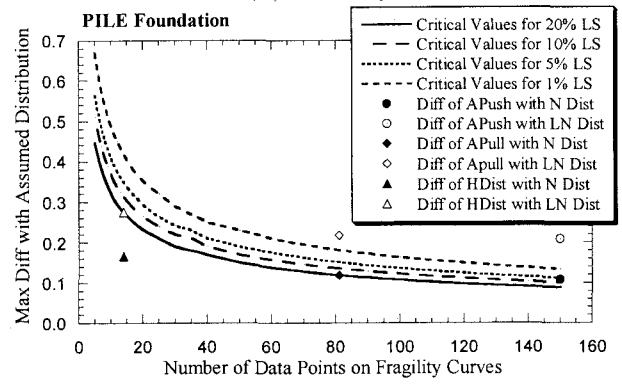

(d) Pile foundation

Note: TSS=Tensile stress in reinforcing steel; BCC=bending compressive stress in concrete; SCC=shear stress in concrete; APush=axial force of push-in; Apull=axial force of pull-out; HDist=Horizontal displacement at pile head; Diff=difference; N Dist=normal distribution; LN Dist.=Lognormal distribution.

Fig. 6 Kolmogrov-Smirnov test results

ure, the fundamental random variables affecting each design criterion are marked.

The tensile failure of reinforcing steel is the most critical mode in pier as shown in Fig. 7(a). The reason is that at any level of ground acceleration the probability of damage for this mode is higher than the other modes. Furthermore, it can be seen from Fig. 8 that this mode is affected by the tensile strength of reinforcing steel that is less variable than the other random variables. In contrast, the bending compressive stress and shear stress in concrete are affected by the compressive strength of concrete, which possesses higher variability than the tensile strength of reinforcing steel. Due to lower variability of the affecting random variables, the tensile stress in reinforcing steel exhibits lower variability than the other two design criteria in pier.

In the fragility curves for footing shown in Fig. 7(b), the bending stress in concrete is of higher reliability than other criteria, because the thickness of the footing is larger than that required to satisfy the design equations for bending compressive stress in concrete. In addition, this mode possesses the largest variability which can be explained in more detail using Fig. 8 as, (1) the mean value of fragility curve of this mode is larger than any other mode as explained before; (2) the affecting random variables are of higher variability than those affecting the tensile stress in reinforcement.

For pile body, the bending compressive stress in concrete is the most reliable mode of failure and of higher variability than the other modes, as shown in Fig. 7(c). A reason of the higher variability of this mode can be explained in a similar way to that of pier. However, the shear stress in pile is seen to be the most critical mode.

Fig. 7(d) shows the fragility curves of pile foundation. In this case, the horizontal displacement at the pile top is observed to be the most critical mode. The axial force of push-in is more critical than that of pull-out at lower level of ground acceleration. However, it becomes the most reliable when the ground acceleration is more than 0.875g. In fact, this limit value of the ground acceleration is more than the upper limit of the L1 earthquake.

In addition, the fragility curve of axial force of push-in has the highest variability in all design criteria that is seen from Fig. 8. One can also see that end bearing resistance and side resistance are effective for axial force of push-in. Due to combined effect of highly variable end bearing and side frictional resistance of pile, such a high variability in the push-in is observed. Comparing with axial force of pull-out, only one additional random variable, which is the end bearing resistance of pile is active in axial force of push-in.

8. Failure Probability

Lifetime failure probabilities P_f for different design criteria are estimated in order to assess the safety levels quantitatively. It is done by convoluting the fragility curves with the probability distribution function (PDF) of seismic hazards for 50 years maximum values of ground acceleration.

8.1 Uncertainty in earthquake ground motion

In order to consider the uncertainty of earthquake force, the method proposed by Kanda and Dan[34] is adopted in this study. They evaluated the uncertainty of earthquake force in terms of the areal average earthquake velocity at the bedrock v_{est} by compiling a large earthquake catalogue and by fitting those data to an extreme value distribution with the lower

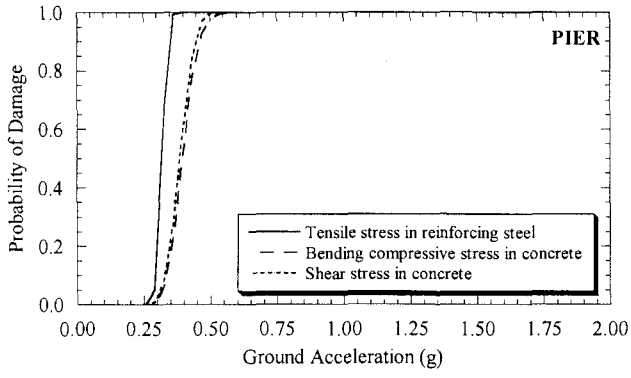

(a) Pier

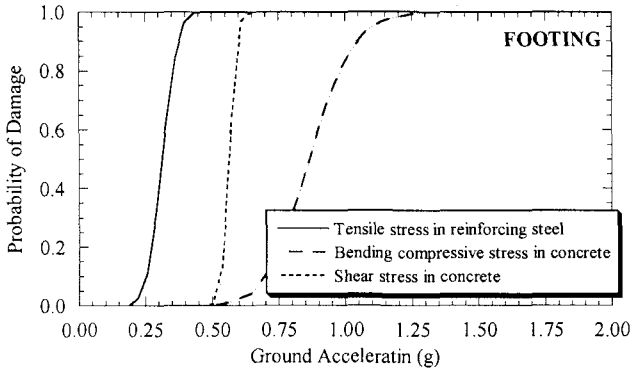

(b) Footing

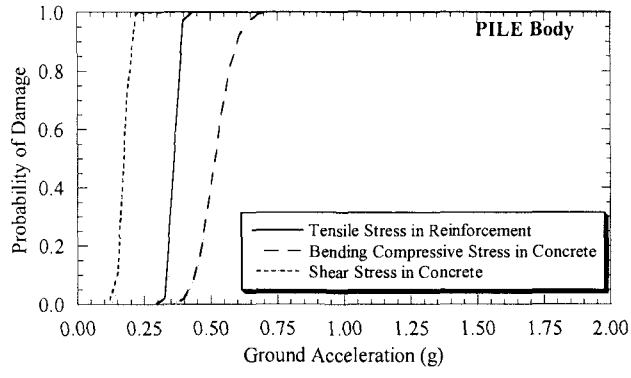

(c) Pile body

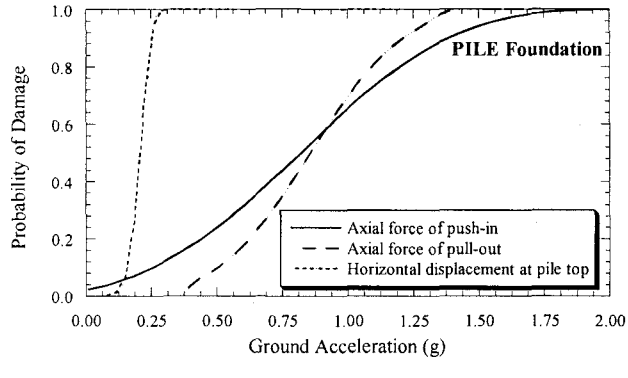

(d) Pile foundation

Fig. 7 Fragility curves for the highway bridge substructure

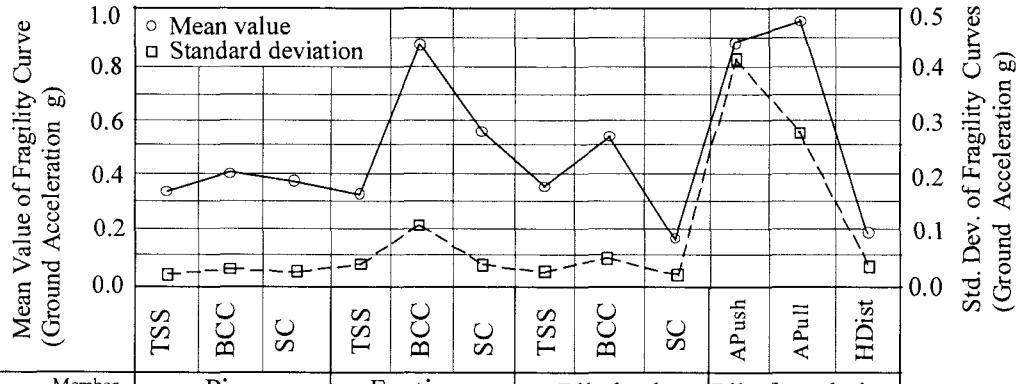

Random variables \ Member	Pier			Footing			Pile body			Pile foundation		
SOIL												
Unit weight (in-situ)							○	○	○	○	○	○
Unit weight (fill)				○	○	○	○	○	○	○	○	○
SPT *N*-value							○	○	○	○	○	○
Side resistance										○	○	
End bearing resistance										○		
REINFORCEMENT												
Tensile strength	○			○			○					
Modulus of elasticity	○	○		○	○		○	○				
CONCRETE												
Unit weight	○	○	○	○	○	○	○	○	○	○	○	○
Modulus of elasticity	○	○		○	○		○	○				
Compressive strength		○	○		○	○		○	○			

Note: TSS: tensile stress in reinforcing bar; BCC: bending compressive stress in concrete; SC: shear stress in concrete; APush: axial force of push-in; APull: axial force of pull-out; and HDist: horizontal displacement at pile top.

Fig. 8 Statistical parameters of the fragility curves with list random variables affecting the fragility curves for different design criteria and members item by item.

and upper limits. The areal average velocity v_{est} implies the estimated average bedrock earthquake velocity over some area. The relationship between the peak ground acceleration and v_{est} proposed by Kanai *et al.*[35] is used for this study. It is given by

$$a_{\max} = \frac{10\pi v_{est}}{\sqrt{T_g}} \tag{14}$$

where T_g = natural frequency of the ground.

Based on Eq. (14), Honjo *et al.*[27] developed the following relationship to estimate peak ground acceleration on stiff ground in Tokyo area,

$$a_{\max} = 47.4 v_{est} \tag{15}$$

The parameters a_{max} and v_{est} estimated for Tokyo area and the 50-year maximum value are employed in the present analysis.

8.2 Numerical results

Fig. 9 shows the estimated values of failure probability in 50 years for all design criteria. It can be seen from Fig. 9 that P_f values fall within a very wide range, ranging from 0.0001 to almost 1. However, for pier P_f values lie within a relatively narrow range (0.09-0.11). The variation for different modes in footing is quite wider, ranging from 0.0001 to 0.12. The minimum value is for bending compressive stress in concrete. The reason for it has been described in Chapter 7. In the case of pile body, the maximum value is for the shear stress in concrete, which is almost equal to one. For the pile foundation, the smallest value of P_f is observed for the axial force of pull-out which is around 10^{-3}. However the maximum value is for the horizontal displacement at pile top and it is around 0.5.

Furthermore, it should be noted from Fig. 9 that the values of P_f for the tensile stress in reinforcement are within a very narrow range (0.1-0.11) in different members. However, it varies significantly in different members for the bending and shear stresses in concrete. For bending compressive stress in concrete,

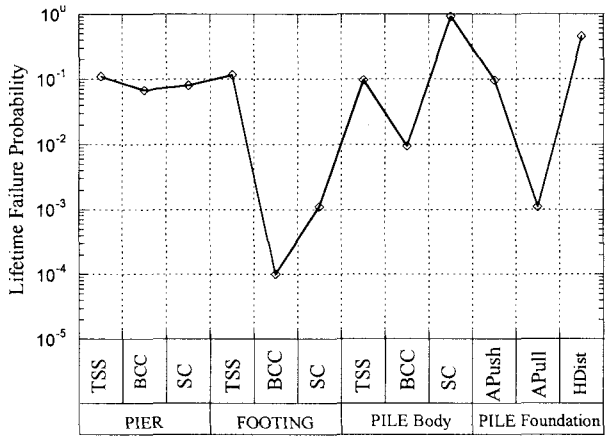

Fig.9 Lifetime failure probability for different members and design criteria

this range is around 0.0001-0.1, while the same for shear stress in concrete is 0.0011-0.9.

9. Member safety factor

In the current work, the material safety factors for concrete and reinforcing steel are considered as 1.3 and 1.1, respectively. It is clear from discussion of the previous chapters that different design criteria in different members have different levels of safety. However, ISO 2394[7] recommends for a uniform level of safety. To do this, we adjust the member safety factor (MSF) on the resistance side of the design equation. To propose the value of MSF, it is necessary to calibrate the safety level by evaluating the failure probability for a large number of bridge's substructures and for wide variety of material parameters. Nevertheless, in order to propose a method of determination of the safety factors, attempts are made to show the relationships between the failure probability and the member safety factors for the substructure considered in this study. In this chapter, first of all, a number of bridges have been designed for different values of MSF. After that the failure probabilities are evaluated for those MSF. Fig. 10 shows the shift of the fragility curves for three different design criteria of pier with the variation of the member safety factors. It is seen from Fig. 10 that fragility curves for all three criteria of pier are shifted towards the right direction. However, the change in variability of the fragility curves is different for different design criteria. From Fig. 10(a), no significant increase in the variability of the tensile stress in reinforcing steel is observed. However, remarkable increase in the variability of the fragility curves is observed for the bending compressive stress in concrete.

Fig. 11 shows the relationships between the failure probabilities and MSF. The rate of change of failure probability is different for three different design criteria. For pier, the failure probability for the bending compressive stress in concrete is found to decrease faster than the other two modes as shown in Fig. 11(a).

In order to propose the numerical values of the member safety factors, the recommendations of ISO 2394[7] is followed for target level of failure probability. The consequences of failure of a design criterion to remain within elastic limit have been considered as moderate and the relative cost of safety measures is taken as high. For these conditions, target level of lifetime failure probability is set at 10^{-2}. For pier, the values of MSF for tensile stress in reinforcing steel, bending compressive and shear stresses in concrete are 1.57, 1.3, and 1.58, respectively. However, the values for bending and shear stresses in concrete for footing cannot be considered because, the value of failure probability is less than the target one for MSF=1.0. The reason is that the thickness of footing is designed to treat it as a rigid body, and hence, it is larger than that required to satisfy the concerned design equation which was discussed Chapter 7.

For pile body, as seen from Fig. 11(c) that the values of MSF for tensile stress in reinforcing steel and bending compressive are 1.38 and 1.05, respectively which fall within the expected level of the values of MSF.

An MSF value for axial load bearing capacity against push-in is found to be around 1.6. However, MSF for axial force of pull out cannot be considered for the same reason as explained for bending compressive and shear stresses in concrete.

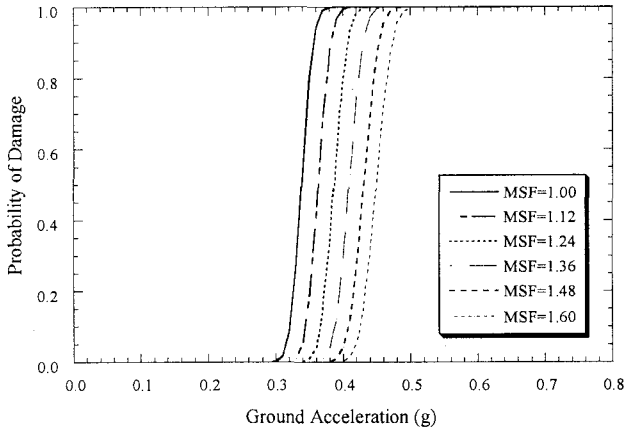

(a) Tensile stress in Reinforcing Steel

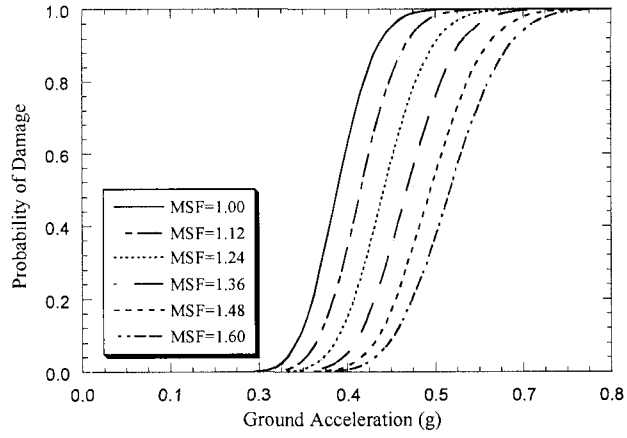

(b) Bending stress in concrete

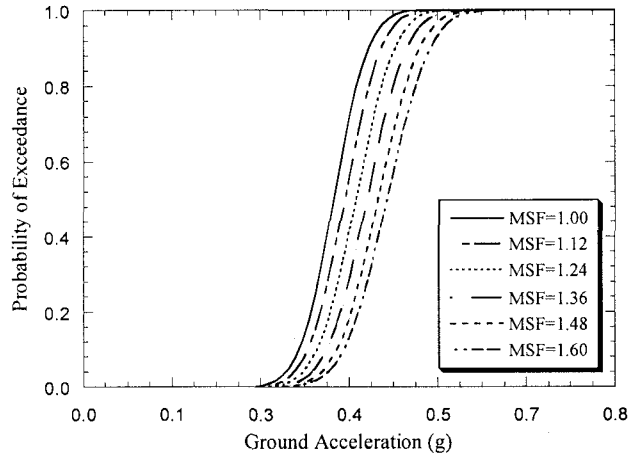

(c) Shear stress in concrete

Fig. 10 Shifting of fragility curves of pier with member safety factors

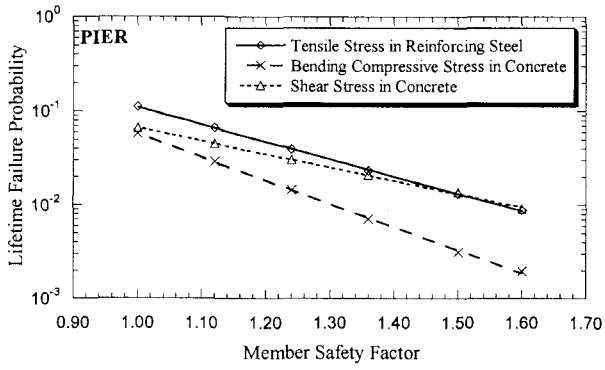

(a) Pier

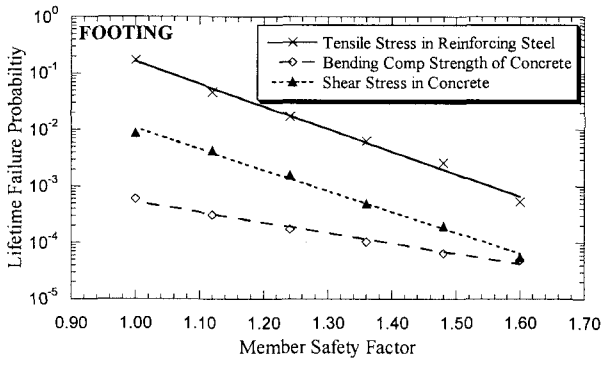

(b) Footing

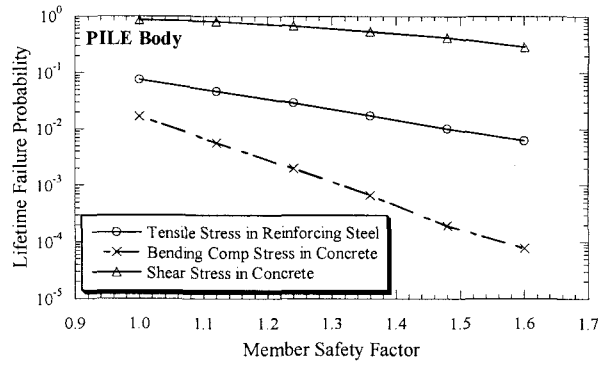

(c) Pile body

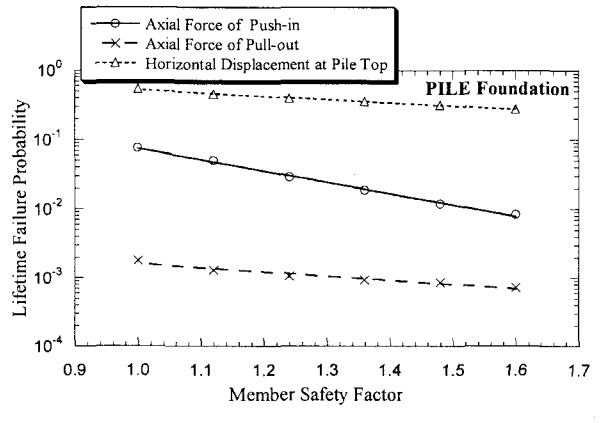

(d) Pile foundation

Fig. 11 Relationship between member safety factors and failure probability

10. Conclusions and further remarks

The main objective of this study is to propose a method of determination of safety factors based on reliability analyses. In order to describe the way of our considerations a bridge substructure is selected as a model. The fragility curves for that model bridge under Level-1 earthquake ground motions have been constructed by using the Monte Carlo simulation.

The following conclusions are drawn for the present study.

Due to higher variability of the random variables related to soil, the variability of the fragility curves for load bearing capacity of pile have been found to be very high as compared to other design criteria in different members. For instance, the standard deviation of fragility curves for axial force of push-in and pull-out are around 0.4 and 0.27, respectively. In contrast, the largest value for the other members is around 0.1.

The Kolmogrov-Smirnov test results indicated that the lognormal distribution, as assumed by many researchers for developing fragility curves, is not followed by the fragility curves for Level-1 earthquakes simulated in this study. Rather the normal distribution is more suitable to approximate the fragility curves.

Remarkable variations of the failure probabilities are found for different design criteria within a member except for pier. For instance, in footing, the maximum value of failure probability is around 0.1 for the tensile stress in reinforcing steel, while that for the bending compressive and shear stresses of concrete are 10^{-4} and 10^{-3}, respectively. However, the variation in pier lies within a very narrow range (i.e., 0.08-0.11).

It is observed that large variation of the failure probabilities exists for same design criteria and different members except for tensile stress in reinforcing steel. As an example, the bending stress in concrete ranges from 10^{-4} to 0.07. However, the failure probabilities for the tensile stress in reinforcing steel in different members lie within a very narrow range (0.09-0.11).

As stated in chapter 2, establishment of a rational procedure to determine safety factors is the major concern of this study. Consequently, other issues such as obtained values for the member safety factors, the accuracy of design equation, and the model itself have been dealt with secondary importance.

It should be noted that the above conclusions are obtained only for a particular bridge and a set of material properties. To make the conclusions more comprehensive, a large number of bridges for a variety of material properties should be studied. This is a future work to be carried out.

References

1) EuroCode 8, Design Provisions for earthquake resistance of structures, European Standards, Brussels, 1994.
2) Caltrans, Seismic Design Criteria, Ver 1.1, California Department of Transport, Sacramento, CA., USA, 1999.
3) JSCE, Earthquake resistant design codes in Japan, *Japan Society of Civil Engineers*, 2000.
4) JRA, Specifications for highway bridges, Part V: Seismic Design, *Japan Roadway Association*, 1996.

5) EuroCode 7, Design Provisions for geotechnical design, Part1: general rules, European Standards, Brussels.
6) Mirza, S. A., Reliability-based design of reinforced concrete columns, *Structural Safety,* 18(2-3), pp. 179-194, 1996.
7) ISO (International Organization for Standardization), 2394, General principles on reliability for structures, 1998.
8) Phoon, K-K., Kulhawy, H. and Grigorio, M. D., Reliability-based design for transmission line structure foundations, *Computers and Geotechniques,* 26(3-4), pp. 169-185, 2000.
9) Kim, S-H. and Feng, M. Q., Fragility analysis of bridges under ground motion with spatial variation, *International J. Non-Linear Mechanics*, 38(5), pp. 705-721, 2003.
10) Karim, K. R. and Yamazaki, F., Effect of earthquake ground motions on fragility curves of highway bridge piers based on numerical simulation, *Earthquake Engineering and Struct. Dyn.,* 30(10), pp. 1839-1856, 2001.
11) Shinozuka M., Feng M. Q., Kim H-K. and Kim, S-H., Nonlinear static procedure for fragility curve development, *J. Eng. Mech.,* ASCE, 126(12), pp.1287-1295, 2000.
12) Ichii, K., A seismic risk assessment procedure for gravity type quay walls, *J. Struct. Mech. and Earthquake Eng.*, JSCE, 9-717(I-61), pp. 13-22, 2002.
13) Shinozuka, M., Grigorio, M., Ingraffea, A. R., Billington, S. L., Feenstra, P., Soong, T. T., Reinhorn, A. M., and Maragakis, E., Development of fragility information for structures and nonstructural components, *Technical reports, National Science Foundation, Earthquake Engineering Research Centers Program*, Federal Highway Administration, pp. 15-32, 2002.
14) Yamzaki, F., Motomura, H. and Hamada, T., Damage assessment of expressway networks in Japan based on seismic monitoring, *12th World Conference on Earthquake Engineering*, CD-ROM, 2000.
15) Shinozuka, M., Lee, J. and Naganuma, T., Statistical analysis of fragility curves, *J. Eng. Mech.,* ASCE, 126(2), pp. 1224-1231, 2000.
16) JRA, Specifications for highway bridges, Part IV: Substructures, *Japan Roadway Association,* 1996.
17) JRA, Reference for seismic design of highway bridges, *Japan Roadway Association*, 1997.
18) Frangopol, D. M., Ide, Y., Spacone, E. and Iwaki, I., A new look at reliability of reinforced concrete columns, *Structural Safety*, 18(2-3), pp. 123-150, 1996.
19) Mirza, S. A., Hatzinikolas, M. and MacGregor, J. G., Statistical descriptions of strength of concrete, *J. Struct. Div.*, ASCE, 105(ST6), pp. 1021-1037, 1979.
20) Low, H. Y. and Hao, H., Reliability analysis of reinforced concrete slabs under explosive loading, *Structural Safety,* 23(2), pp. 157-178, 2001.
21) Galambos, T.V. and Ravindra, M. K., Properties of Steel for Use in LRFD, *J. Struct. Div.*, ASCE, 104 pp. 1459-1468, 1978.
22) Mirza, S. A. and MacGregor, J. G., Variability of mechanical properties of reinforcing bars, *J. Struct. Div.*, ASCE, 105(ST56), pp. 921-937, 1979.
23) Arafah A. M., Statistics of concrete and steel quality in Saudi Arabia, *Magazine of Concrete Research*, 49(180), pp. 185-193, 1997.
24) Kulhawy, F. H., On the evaluation of soil properties, *Geotechnical special publication,* No. 31, ASCE, pp. 95-115, 1992.
25) Phoon, K. K. and Kulhawy, F. H., Characterization of geotechnical variability, *Canadian Geotech. J.*, 36, pp. 612-624, 1999.
26) Rackwitz, R., Reviewing probabilistic soil mechanics, *Computers and Geotechnics*, 26(3-4), pp.199-223, 2000.
27) Honjo, Y., Suzuki, M., and Matsuo, M., Reliability analysis of shallow foundations in reference to design codes development, *Computers and Geotechnics*, 26(3-4), pp. 331-346, 2000.
28) Vanmarcke, E., Probabilistic modeling of soil profiles, *J. Geotech.*, ASCE, 103(GT11), pp. 1227-1246, 1977.
29) Honjo, Y., Suzuki, M., Shirato, M. and Fukui, J., Determination of partial factors for a vertically loaded pile based on reliability analysis, *Soils and Foundations*, 42(5), pp. 91-109, 2002.
30) Al-Harthy, A. S. and Frangopol, D. M., Reliability based design of prestressed concrete beams, *J. Struct. Eng.*, ASCE, 120(11), pp. 3156-3177, 1994.
31) Duncan, J. M., Factors of safety and reliability in Geotechnical Engineering, *J. Geotech. And Geoenv. Eng.*, ASCE, 126(4), pp. 307-316, 2000.
32) Wolfarm, S., The Mathematica, 4th Edition, Cambridge University Press, 1999.
33) Haldar, A., and Mahadevan, S., *Probability, reliability and statistical methods in engineering design*, John Wiley & Sons, Inc., 2000.
34) Kanda, J. and Dan, K., Distribution of seismic hazard in Japan based on empirical extreme value distribution, *Structural Safety*, 3(4), pp. 229-239, 1987.
35) Kanai *et al.*, Observation of strong earthquake motions in Matsuhiro area, part. *Bull. earthq. Rs. Inst.*, 44, pp. 1269-1296, 1966.

(Received on September 12, 2003)